

# A Molecular Descriptor for Characterizing the Strength of Through-Space Conjugation for Luminescent Property in Organic Materials

Published as part of *The Journal of Physical Chemistry Letters* special issue "Wei-Hai Fang Festschrift".

Meihui Liu, Wei Wang, Peifeng Su, Jiajun Ren, and Qian Peng\*



Cite This: *J. Phys. Chem. Lett.* 2025, 16, 8731–8738



Read Online

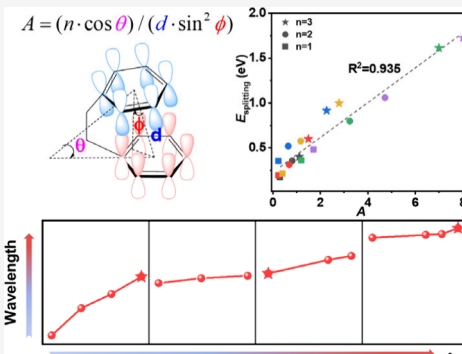
ACCESS |

Metrics & More

Article Recommendations

Supporting Information

**ABSTRACT:** Noncovalent through-space conjugation (TSC), a unique property of  $\pi$ -charge delocalization, has emerged as a powerful strategy for modulating the optoelectronic properties of organic materials. However, the quantitative relationship among the molecular structure, the strength of TSC, and optoelectronic properties has not yet been established. Here, using typical conjugated aromatic compounds as model systems, it is revealed that TSC arises from the interaction of  $\pi$ -orbitals, and a molecular descriptor, composed of geometric parameters, is proposed to characterize the strength of TSC. This descriptor exhibits a strong linear correlation with the orbital splitting energy of symmetric and antisymmetric  $\pi$ -orbitals, achieving a linear fit coefficient ( $R^2$ ) as high as 0.935. More importantly,  $A$  shows a strong positive correlation with the spectral red-shift of organic materials, suggesting that TSC can effectively tune the luminescent properties of organic materials. The descriptor is helpful for the rational design and machine-learning-based high-throughput screening of advanced organic luminescent materials.



In recent years, tuning of intramolecular noncovalent interactions has emerged as a significant method to modulate the optoelectronic properties of organic materials.<sup>1–4</sup> Herein, through-space conjugation (TSC) is a noncovalent interaction between aromatic rings with  $\pi$  electron delocalization.<sup>5</sup> It has been gradually proved as an important strategy for enhancing optoelectronic properties, such as aggregation-induced emission (AIE), circularly polarized luminescence (CPL), multichannel conductance, high charge mobility, and so on.<sup>6–18</sup> For example, the strength of TSC in trinaphthylmethane isomers was found to increase with the number of naphthalene units, and the strong TSC induced highly efficient long-wavelength clusteroluminescence with an impressive quantum efficiency of 55%.<sup>6</sup> By combining free radicals coupled with strong TSC, a remarkable full-spectrum emission spanning from blue to near-infrared (NIR) has been achieved.<sup>7</sup> The chiral foldamers tailored by TSC exhibit reversibly switchable dual circularly polarized luminescence with opposite signs at different emission wavelengths.<sup>12,13</sup> TSC enabled the construction of single-molecule wires with multichannel conductance, compensating for conductivity losses caused by poor conjugation through bonds.<sup>14–17</sup> For phenanthrene derivatives, the electron mobilities of folded molecules with TSC are 3 orders of magnitude higher than those of widely used linear and planar ones.<sup>18</sup> It can be seen from the above findings that adjusting the strength of TSC has a significant impact on the optoelectronic properties. Many efforts have been made to strengthen TSC, such as introducing

electron-donating groups,<sup>19</sup> increasing the conjugated chain length,<sup>20,21</sup> and expanding the number of benzene rings on the conjugated plane.<sup>22</sup> However, a direct quantitative relationship among molecular structure, TSC strength, and optoelectronic properties has not yet been established, which hampers the rational design and high-throughput screening of high-performance optoelectronic materials.

Tracing the development history of TSC in theory, Hoffmann first proposed the concept of through-space interaction (TSI) in 1968, defining it as the interaction of orbitals among radical lobes in the same molecule separated by a number of intervening  $\sigma$  bonds and describing its strength using the energy splitting.<sup>23,24</sup> The study of TSI began with the di-*p*-xylylene structure, where two phenyl rings face each other and the  $\pi$ -electrons are delocalized between closely aligned benzene rings.<sup>25</sup> The distance between the two rings (3.09 Å) is shorter than the sum of the van der Waals radii (3.40 Å) of the atoms involved,<sup>26</sup> and the energy gap (3.72 eV) between the highest occupied molecular orbital (HOMO) and the lowest unoccupied molecular orbital (LUMO) is much smaller

Received: July 22, 2025

Revised: August 8, 2025

Accepted: August 13, 2025

Published: August 19, 2025



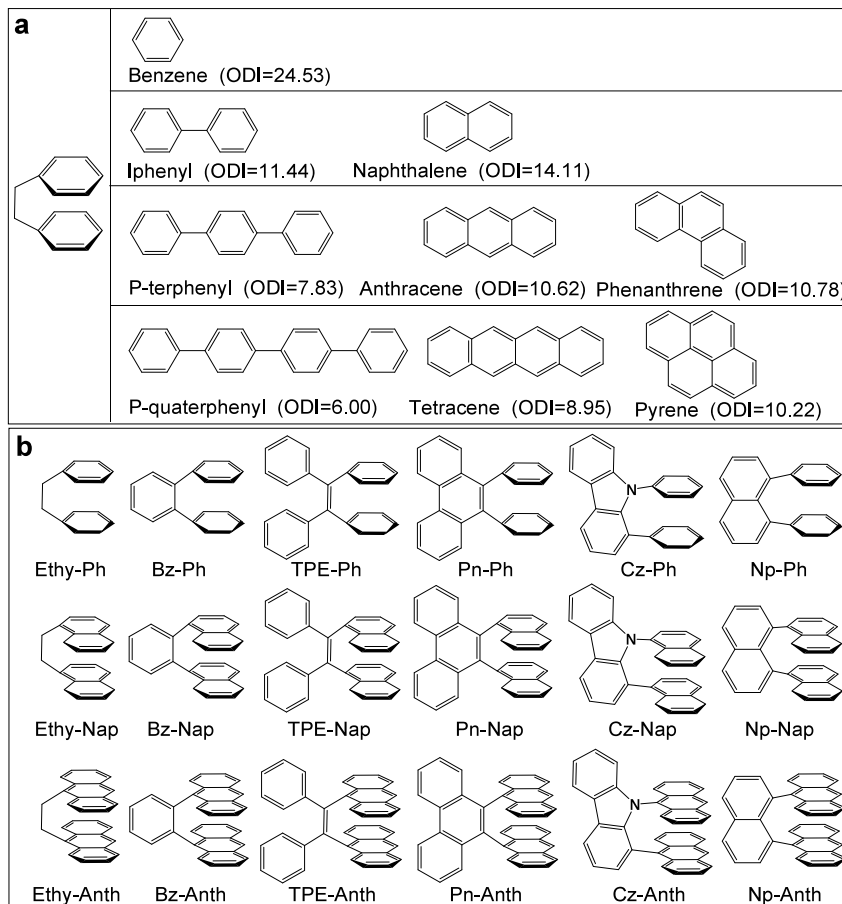


**Figure 1.** (a) Molecular models for TSC with orbital delocalization indices (ODIs). (b) Molecular structures for 18 compounds, using 1,2-ethanediyl (Ethy), benzene (Bz), (*Z*)-1,2-diphenylethene (TPE), phenanthrene (Pn), carbazole (Cz), and naphthalene (Np) as bridging units, respectively.

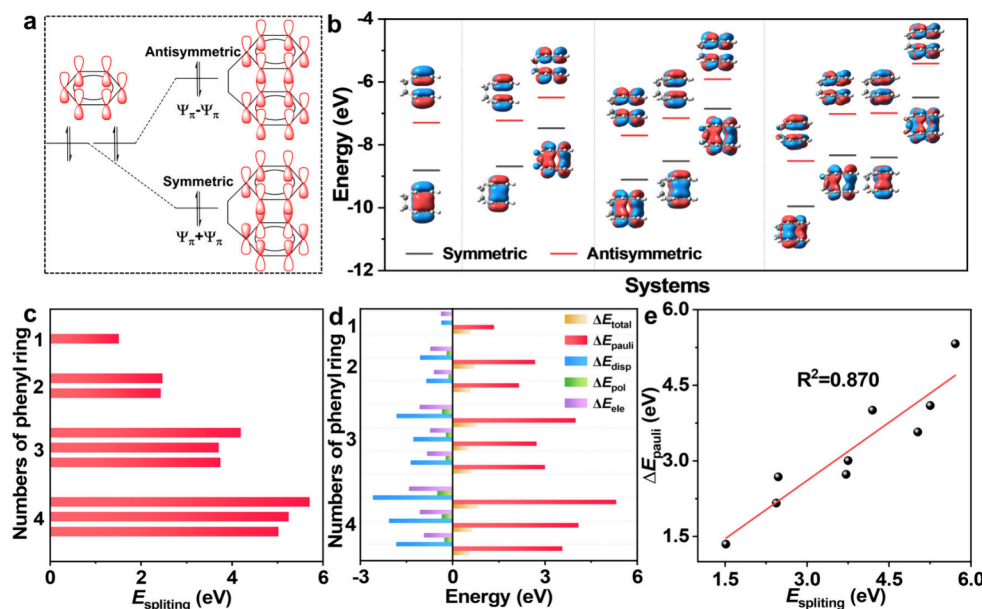


**Figure 2.** (a) TSC illustrated by orbital interaction; (b) The energies and charge distributions of the symmetric and antisymmetric  $\pi$  orbitals (Isosurface = 0.02 a.u.); The  $x$ -axis corresponds to systems with  $\pi$ -groups being benzene, naphthalene, anthracene, and tetracene, arranged from left to right. (c) The  $E_{\text{splitting}}$  of these orbitals; and (d) The generalized Kohn–Sham energy decomposition analysis (GKS-EDA) results, which is described in [Supplementary Notes S2](#); The  $y$ -axis corresponds to increasing number of phenyl rings and ODI value. (e) The correlation between  $E_{\text{splitting}}$  and  $\Delta E_{\text{pauli}}$  for these studied molecular models.

than that of single benzene (5.15 eV). These all suggested the existence of TSI.<sup>27–29</sup> TSI in cyclophanes is considered as the competition between the attractive (dispersive and electrostatic) interactions and the repulsive interactions.<sup>30</sup> Many studies also suggest that the essence of TSI comes from orbital interaction in aromatic ring systems.<sup>31–33</sup> In the context of TSI, the term “through-space conjugation” first appeared in 2011,<sup>34</sup> and it was formally defined using f-TPE-PPy as an example in 2015.<sup>16</sup> Although TSC has been applied to achieve excellent optoelectronic properties, it has not been investigated systematically in theory, and its intrinsic nature of TSC remains underexplored.

In this work, it is revealed from first-principles calculations that the TSC stems from the interaction of  $\pi$ -orbitals in organic molecules, and a descriptor  $A$ , composed of geometrical parameters (including the number of conjugated rings, centroid distance, dislocation angle, and dihedral angle), is proposed to characterize the strength of TSC. This descriptor not only behaves a strong linear relationship with the splitting energy between symmetric and antisymmetric  $\pi$ -orbitals but also exhibits a good positive correlation with both the spectral redshift of organic materials.

Conjugation refers to the overlap or sharing of the orbitals of atoms or groups, resulting in the delocalization of charges across a system of connected atoms and groups. Through-bond conjugation (TBC) is very common in organic molecules, especially organic aromatic molecules, whereas TSC occurs only when two conjugated  $\pi$ -groups are close enough to each other in space. Keeping this in mind, we constructed a molecular model in which two methylene groups were used as a bridge and two  $\pi$ -groups were symmetrically connected in a face-to-face manner at a constant perpendicular distance of 3.10 Å, less than the sum of van der Waals radii (3.40 Å) (Figure 1a). The  $\pi$ -groups were appointed as benzene derivatives with different degrees of charge delocalization, which can be measured by orbital delocalization index (ODI),<sup>35,36</sup> which is described in Supplementary Notes S1. The larger the ODI value, the weaker the degree of electron delocalization. It can be found in Figure 1a that as the number of phenyl rings ( $n$ ) increases, the degree of charge delocalization strengthens with a decreasing ODI value. For the models with the same number of phenyl rings (e.g.,  $n = 4$ ), the degree of charge delocalization decreases from *p*-quaterphenyl to tetracene and then pyrene due to the shortened conjugated length.

Based on Hoffmann’s orbital theory in Figure 2a, the strength of TSC is gauged by the splitting energy between symmetric and antisymmetric orbitals formed by  $\pi$ -orbital interactions.<sup>37</sup> The symmetric and antisymmetric orbitals of the molecular models were obtained at the level of M062X-(D3)/6–31+G(d) and plotted in Figure 2b, and the resultant splitting energies ( $E_{\text{splitting}}$ ) are shown in Figure 2c. It can be noticed in Figure 2b that with an increasing number of phenyl rings, more than one pair of symmetric and antisymmetric orbitals are formed owing to the participation of the bridges. In this case,  $E_{\text{splitting}}$  is the energy difference between the symmetric and antisymmetric highest occupied orbitals. It is easily seen in Figure 2c that the  $E_{\text{splitting}}$  gradually rises with the increase of the number of phenyl rings, and for the models with the same number of phenyl rings (taking  $n = 4$  as example) it decreases from *p*-quaterphenyl to tetracene and then pyrene because the charge delocalization is reduced in the same order. These indicate that the  $\pi$ -orbital interactions make

the molecules with a higher degree of charge delocalization more stable. As it is also known that the Pauli repulsion is defined as an interaction between occupied orbitals,<sup>38,39</sup> whose energy ( $\Delta E_{\text{pauli}}$ ) can be calculated using the energy decomposition analysis (EDA) method.<sup>40</sup> In these molecular models,  $\Delta E_{\text{pauli}}$  is dominant among the decomposed energy terms of total TSI ( $\Delta E_{\text{pauli}}$ ,  $\Delta E_{\text{disp}}$ ,  $\Delta E_{\text{pol}}$ , and  $\Delta E_{\text{ele}}$ ) (Figure 2d). It can be seen that there is a good linear correlation with fitting index of 0.870 between  $\Delta E_{\text{pauli}}$  and  $E_{\text{splitting}}$  (Figure 2e), which suggests that the strength of TSC can be quantitatively characterized by the two methods. Furthermore, it can be found that TSC is short-range, and its strength decreases rapidly with increasing distance. Beyond a certain distance, the dispersion interaction will become dominant between  $\pi$ -groups, as is commonly discussed in conjugated systems.

To check the effect of electronic effects on the strength of TSC, we introduced different electron-donating and electron-withdrawing groups as well as heteroatoms on the phenyl ring and calculated their  $E_{\text{splitting}}$  and  $\Delta E_{\text{pauli}}$  (Figure S1). The detailed energy decomposition results are shown in Table S1. It is found that relative to TSC in parent benzene, the electron-donating  $-\text{NH}_2$  and  $-\text{SCH}_3$  groups enhance the strength of TSC by providing more electrons to the center of the phenyl ring (Figure S2). In contrast, the electron-withdrawing groups and heteroatoms reduce the strength of TSC because they diminish the electron density of the center of the phenyl ring by pulling electron toward external  $-\text{F}$ ,  $-\text{NO}_2$ , or N atoms. However, the influence of substituents is slight and scarcely considered in the following work.

From the discussion above, it is known that the orbital interaction determines the strength of TSC. Upon careful inspection, several geometric parameters are considered to be highly associated with the orbital overlap integral, including the number of conjugated rings ( $n$ ), the centroid distance between the two  $\pi$ -groups ( $d$ ), the vertical distance ( $z$ ), the dislocation angle ( $\phi$ ), the slip distance ( $a$ ), and the dihedral angle ( $\theta$ ) between two conjugated rings (Figure 3a). Triggered by this, we established a descriptor composed of geometric parameters:

$$A = \frac{n \cdot \cos \theta}{d \cdot \sin^2 \phi} \quad (1)$$

To validate the rationality and reliability of this descriptor, we constructed 18 molecules featuring typical “bridge” structures found in reported TSC systems, with benzene, naphthalene, and anthracene symmetrically connected as the “ $\pi$ -groups” at both ends (Figure 1b). These 18 molecules were optimized using M062X(D3)/6–31+G(d),<sup>41–46</sup> and no imaginary frequencies were observed. To verify the reliability of this method, six molecules were also optimized using the PW6B95(D3)/6–31+G(d), which is reported to perform well for noncovalent systems.<sup>30</sup> A comparison of structural parameters and the calculated  $A$  between the two methods is shown in Figure S3. The consistency in trends supports the validity of using M06–2X(D3)/6–31+G(d) for geometry optimization in this study. The results are provided in Table S2. Based on the optimized structures, the  $A$  values and the orbital interactions  $E_{\text{splitting}}$  were computed and compared with each other, and a strong positive correlation between  $E_{\text{splitting}}$  and  $A$  is found with a linear fit coefficient ( $R^2$ ) up to 0.935 (Figure 3b). For molecules with the same bridge, the  $A$  values gradually increase as the degree of delocalization in the  $\pi$ -groups increases. Among molecules with different bridges, the  $A$  values of those with carbazole and naphthalene bridges (6.99

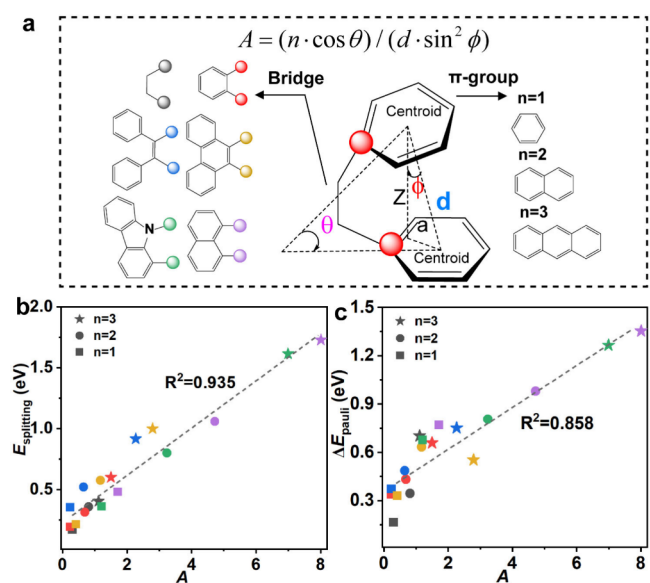


**Figure 3.** (a) The computational model and geometrical parameters for this descriptor; (b) The correlation between  $E_{\text{splitting}}$  and  $A$ ; (c) The correlation between  $\Delta E_{\text{pauli}}$  and  $A$  for 18 compounds. The black, red, blue, yellow, and green represent Ethy-, Bz-, TPE-, Pn-, Cz-, and Np- bridges, respectively, and the squares, circles, and stars represent -Ph, -Nap, and -Anth π-groups, respectively, for these 18 compounds.

and 8.01, respectively) are significantly higher than those with other bridging units. Furthermore, the  $\Delta E_{\text{pauli}}$  values of these molecules were evaluated through EDA method, and the results (Table S3) were compared with the  $A$  values. The resulting  $R^2$  is equal to 0.858, showing a significant linear correlation between  $\Delta E_{\text{pauli}}$  and  $A$ , as shown in Figure 3c. However, this correlation is slightly weaker than that between  $E_{\text{splitting}}$  and  $A$ , which can be attributed to the fact that the interaction between the highest occupied orbitals more directly reflects the intrinsic nature of TSC. So far, the nature of TSC has been explored, and the quantitative relationship has been established between TSC strength and molecular structures.

To disclose a clearer structure-strength relationship, we further investigate the influences of these four structural parameters in eq 1 on  $A$  values in Figure S4 and S5. It is found that (i) when  $n$  is gradually increased from 1 to 3,  $A$  exhibits an almost linear increase, which suggests that  $n$  is a very important parameter in determining the value of  $A$ . (ii) The obvious TSC ( $E_{\text{splitting}} > 0.36$  eV and  $A > 1.00$ ) appears when  $d$  is smaller than 4.20 Å. It is noted that naphthalene and carbazole are two highly effective bridges, providing smaller steric hindrance for two π-groups to approach each other with  $d < 3.68$  Å. (iii) The smaller  $\theta$  and  $\phi$  are, the larger the  $A$  value is, owing to two conjugated rings being aligned in a tighter face-to-face manner. These provide a clear molecule design strategy to achieve strong TSC systems, namely, increasing the number of rings in π-groups and decreasing the degree of distortion between two π-groups through selecting suitable bridges.

The optical spectrum is a fundamental property of organic optoelectronic materials,<sup>47,48</sup> and the absorption spectra of 18 studied compounds were first investigated. The absorption spectra were obtained by evaluating the excitation energies ( $E_{\text{ex}}$ ) of the singlet excited state with the largest oscillator strength based on the optimized geometries (Supplementary Notes S3) in the ground state ( $S_0$ -geometry) and broadening them using the Gaussian function with a full width at half-maximum set to be 30 nm, and they are plotted in Figure 4. The HOMO, LUMO, HOMO–LUMO gap,  $E_{\text{ex}}$  and oscillator strengths of each state are summarized in Tables S4 and S5. It is obviously seen in Figure 4 that in the series of compounds with the same bridge there is always a progressive redshift in the spectra with the increase of the value of  $A$ . However, the values of the red shift are different in different series of compounds. In the series of compounds with Ethy, Bz, and Np bridges, the rate of redshift in the absorption spectrum is faster than that of increase in  $A$  value. In contrast, in the compounds TPE, Pn, and Cz bridges, the wavelengths of absorption spectra increase linearly with increasing  $A$ . In addition, the changes in the wavelength of absorption spectrum and  $A$  value for the compounds with π-groups from -Ph to -Nap are both smaller than those compounds with π-groups from -Nap to

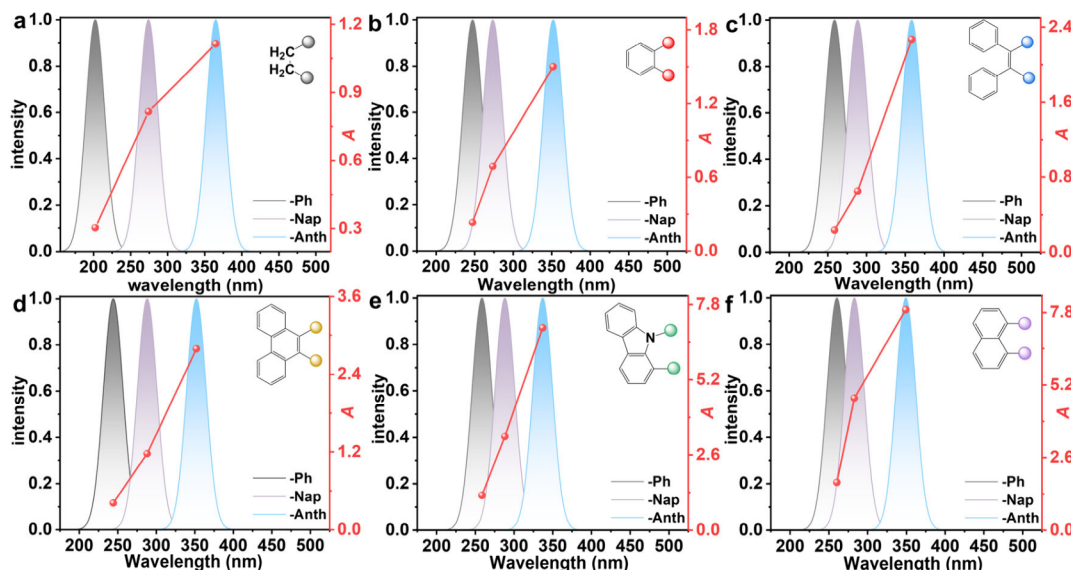


**Figure 4.** Absorption spectra of the compounds with (a) Ethy-, (b) Bz-, (c) TPE-, (d) Pn-, (e) Cz-, and (f) Np- as bridges and -Ph, -Nap, and -Anth as π-groups.

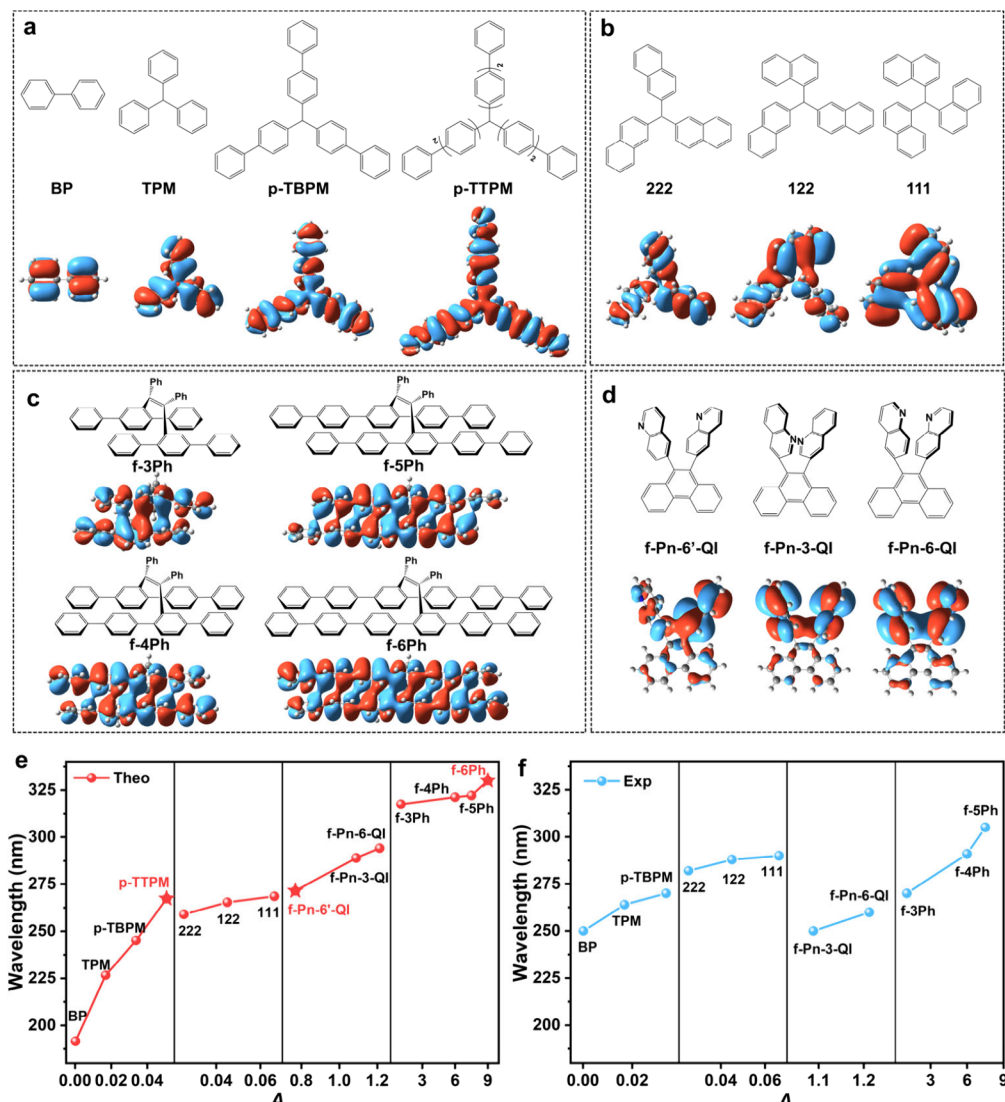


**Figure 5.** (a, b, c, d) Molecular structures and symmetric  $\pi$ -orbitals of the studied compounds; (e, f) Correlation between the absorption wavelength and  $A$ . Red dots and stars denote calculated results for reported and newly designed compounds, respectively, and blue dots correspond to experimental values.

—Anth. Overall, a larger  $A$  correlates positively with  $E_{\text{splitting}}$ , which represents the difference between the symmetric and antisymmetric occupied orbitals. Stronger TSC leads to enhanced  $\pi$ -orbital delocalization, which stabilizes the excited state and reduces the  $E_{\text{ex}}$ . Consequently, the absorption spectrum undergoes redshift. The trend of the change in  $E_{\text{ex}}$  is consistent with the variation in TSC strength. These findings indicate that a direct link is well established from the molecular structure and the strength of TSC to the photophysical properties.

In addition, Kasha's exciton theory has long served as a foundational model for understanding the spectral behaviors of conjugated aromatic chromophores in aggregation.<sup>49</sup> In Kasha's model, the shift in the absorption spectrum of the aggregate relative to that of the monomer is proportional to the excitonic coupling ( $J$ ) between adjacent chromophores. The  $J$  is determined by the magnitude, relative orientation, and distance between their transition dipole moments (Figure S6). To examine whether Kasha's exciton model is adequate to account for the spectral shift observed in the above systems, we further calculated the  $J$  between the two conjugated groups

after removing the bridge and obtained the corresponding absorption energies (Figure S6 and Table S6). The absorption energies predicted by the exciton model are significantly overestimated compared with those obtained by direct calculations on the full molecule. These results suggest that Kasha's exciton theory is not suitable for these systems because it assumes weak electronic coupling and neglects through-bond covalent and through-space noncovalent interactions (namely, TSC, dispersion and electrostatic interactions, and so on) between the two  $\pi$ -conjugated groups.

To demonstrate the applications of the descriptor, we selected the typical organic compounds (Figure 5a–d) with TSC from experiments and newly designed ones, and computed their  $A$  values and absorption wavelengths. As shown in Figure 5e and f, with the increase of the  $A$  value, a clear redshift in the absorption wavelength is observed in both experimental measurements and theoretical predictions. For molecular frameworks with increasing phenyl rings (Figure 5a with  $n = 1–3$  and Figure 5c with  $n = 3–6$ ), the extended  $\pi$ -conjugated groups generate increasingly delocalized orbitals, resulting in greater spatial overlap. Thus, the TSC gets

stronger, leading to a larger  $A$  value, which is consistent with the consequent red shift in the absorption spectrum (Figure 5e). These results are easily referred from the chemical intuition by looking at the molecular structures. Therefore, it is a natural strategy for designing molecules with longer absorption wavelength by adding phenyl ring to extend the  $\pi$ -groups. For the isomer systems with the same number of aromatic rings (Figure 5b and d), subtle changes in connection positions significantly alter absorption wavelengths, making them difficult to intuitively infer from chemical structure alone. From eq 1, it is known that the value of  $A$  is also sensitive to the dislocation angle and the dihedral angle between two conjugated groups, which can be adjusted by changing the linking position of the  $\pi$ -groups on the central bridge and by the substitution of heteroatoms in the  $\pi$ -groups. Excitingly, the values of  $A$  of these systems also exhibit a strong correlation with the absorption wavelengths, as shown in Figure 5f. These indicate that, on one hand,  $A$  can accurately reflect the dependence of TSC strength on molecular structure, and on the other hand, the TSC strength can quantitatively regulate the absorption spectrum in organic systems. Therefore, a clear relationship is established between molecular geometrical structure, the strength of TSC, and the luminescent properties, and the descriptor  $A$  can be used for the rational design and high-throughput screening of excellent luminescent materials.

By using typical conjugated aromatic groups as model systems, first-principles calculations reveal that the TSC arises from the interaction between closely spaced  $\pi$ -orbitals in organic molecules, and its strength can be quantitatively characterized by the splitting energy between symmetric and antisymmetric  $\pi$ -orbitals or the Pauli repulsion interaction. Inferred from this, the strength of TSC largely depends on the geometric structure of the overlapping  $\pi$ -orbitals, including structure parameters such as the number of conjugated rings, the centroid distance, the slip angle, and the spatial dihedral angle between the two related  $\pi$ -groups. Based on these geometric parameters, a descriptor  $A$  is proposed to characterize the strength of TSC,  $A = \frac{n \cdot \cos \theta}{d \cdot \sin^2 \phi}$ . This descriptor can be easily obtained without performing complex quantum chemical calculations. As expected,  $A$  behaves a strikingly linear relationship with the orbital splitting energy ( $R^2 = 0.935$ ) and the Pauli repulsion interaction ( $R^2 = 0.858$ ). Furthermore, this descriptor provides a clear molecular design strategy to achieve strong TSC systems, namely, increasing the number of rings in  $\pi$ -groups and reducing the degree of distortion between two  $\pi$ -groups by selecting suitable bridging structures. Importantly, there is a strong positive correlation between  $A$  and the spectral redshift. Thus, a quantitative relationship is well established among the molecular structure, TSC strength, and luminescent properties. This descriptor  $A$  is a powerful tool for understanding and predicting the optoelectronic properties of organic compounds with TSC, enabling the rational design and large-scale high-throughput screening of high-performance luminescent materials.

## METHODS

All the geometrical and electronic structures of the investigated system in the ground state were calculated at M062X(D3)<sup>41</sup> of theory using the basis set 6-31+G(d) in the Gaussian 16 program.<sup>50</sup>

GKS-EDA calculations were performed with XEDA<sup>51</sup> interfaced with the GAMESS program.<sup>52</sup> The fragmentation

scheme,<sup>40</sup> which is presented in the Supporting Information, was used for the GKS-EDA study of intramolecular interactions in the model molecules in Figure 1.

## ASSOCIATED CONTENT

### Supporting Information

The Supporting Information is available free of charge at <https://pubs.acs.org/doi/10.1021/acs.jpcllett.5c02266>.

Detailed description of the computational methods, energy decomposition analysis results, optimized geometries, and key structural parameters of the studied molecules, as well as data on frontier molecular orbital energies, HOMO–LUMO gaps, excited state energies, and oscillator strengths (PDF)

## AUTHOR INFORMATION

### Corresponding Author

**Qian Peng** – School of Chemical Sciences, University of Chinese Academy of Sciences, Beijing 100049, P. R. China;  [orcid.org/0000-0001-8975-8413](https://orcid.org/0000-0001-8975-8413); Email: [qianpeng@ucas.ac.cn](mailto:qianpeng@ucas.ac.cn)

### Authors

**Meihui Liu** – School of Chemical Sciences, University of Chinese Academy of Sciences, Beijing 100049, P. R. China

**Wei Wang** – The State Key Laboratory of Physical Chemistry of Solid Surfaces, College of Chemistry and Chemical Engineering, Fujian Provincial Key Laboratory of Theoretical and Computational Chemistry, Xiamen University, Xiamen, Fujian 361005, China

**Peifeng Su** – The State Key Laboratory of Physical Chemistry of Solid Surfaces, College of Chemistry and Chemical Engineering, Fujian Provincial Key Laboratory of Theoretical and Computational Chemistry, Xiamen University, Xiamen, Fujian 361005, China;  [orcid.org/0000-0003-4398-6888](https://orcid.org/0000-0003-4398-6888)

**Jiajun Ren** – Key Laboratory of Theoretical and Computational Photochemistry, Ministry of Education, College of Chemistry, Beijing Normal University, Beijing 100875, China;  [orcid.org/0000-0002-1508-4943](https://orcid.org/0000-0002-1508-4943)

Complete contact information is available at: <https://pubs.acs.org/10.1021/acs.jpcllett.5c02266>

### Notes

The authors declare no competing financial interest.

## ACKNOWLEDGMENTS

The authors acknowledge the financial support from the National Natural Science Foundation of China (Grant Nos. 22325305 and 22273105), the Strategic Priority Research Program of Sciences (XDB0520103), National Key R&D Program of China (2024YFB3614300), and the Fundamental Research Funds for the Central Universities (Grant Nos. E2E40307 × 2 and E2ET0309 × 2).

## REFERENCES

- Liu, K.; Zhang, J.; Shi, Q.; Ding, L.; Liu, T.; Fang, Y. Precise Manipulation of Excited-State Intramolecular Proton Transfer via Incorporating Charge Transfer toward High-Performance Film-Based Fluorescence Sensing. *J. Am. Chem. Soc.* **2023**, *145*, 7408–7415.
- He, B.; Zhang, S.; Zhang, Y.; Li, G.; Zhang, B.; Ma, W.; Rao, B.; Song, R.; Zhang, L.; Zhang, Y.; He, G. ortho-Terphenylene Viologens with Through-Space Conjugation for Enhanced Photocatalytic

- Oxidative Coupling and Hydrogen Evolution. *J. Am. Chem. Soc.* **2022**, *144*, 4422–4430.
- (3) Neel, A. J.; Hilton, M. J.; Sigman, M. S.; Toste, F. D. Exploiting Non-Covalent  $\pi$  Interactions for Catalyst Design. *Nature*. **2017**, *543*, 637–646.
- (4) Zhang, J.; Alam, P.; Zhang, S.; Shen, H.; Hu, L.; Sung, H. H. Y.; Williams, I. D.; Sun, J.; Lam, J. W. Y.; Zhang, H.; Tang, B. Z. Secondary through-space interactions facilitated single-molecule white-light emission from clusteroluminogens. *Nat. Commun.* **2022**, *13*, 3492.
- (5) Yang, S. Y.; Qu, Y. K.; Liao, L. S.; Jiang, Z. Q.; Lee, S. T. Research Progress of Intramolecular  $\pi$ -Stacked Small Molecules for Device Applications. *Adv. Mater.* **2022**, *34*, No. 2104125.
- (6) Xu, Q.; Zhang, J.; Sun, J. Z.; Zhang, H.; Tang, B. Z. Efficient organic emitters enabled by ultrastrong through-space conjugation. *Nat. Photonics* **2024**, *18*, 1185–1194.
- (7) Zhang, Z.; Xiong, Z.; Zhang, J.; Chu, B.; Liu, X.; Tu, W.; Wang, L.; Sun, J. Z.; Zhang, C.; Zhang, H.; Zhang, X.; Tang, B. Z. Near-Infrared Emission Beyond 900 nm from Stable Radicals in Nonconjugated Poly(diphenylmethane). *Angew. Chem., Int. Ed.* **2024**, *63*, No. e202403827.
- (8) Wang, Y.; Zhang, J.; Xu, Q.; Tu, W.; Wang, L.; Xie, Y.; Sun, J. Z.; Huang, F.; Zhang, H.; Tang, B. Z. Narrowband clusteroluminescence with 100% quantum yield enabled by through-space conjugation of asymmetric conformation. *Nat. Commun.* **2024**, *15*, 6426.
- (9) Guo, J.; Fan, J.; Liu, X.; Zhao, Z.; Tang, B. Z. Photomechanical Luminescence from Through-Space Conjugated AIEgens. *Angew. Chem., Int. Ed.* **2020**, *59*, 8828–8832.
- (10) Zhang, H.; Zheng, X.; Xie, N.; He, Z.; Liu, J.; Leung, N. L. C.; Niu, Y.; Huang, X.; Wong, K. S.; Kwok, R. T. K.; Sung, H. H. Y.; Williams, I. D.; Qin, A.; Lam, J. W. Y.; Tang, B. Z. Why Do Simple Molecules with "Isolated" Phenyl Rings Emit Visible Light? *J. Am. Chem. Soc.* **2017**, *139*, 16264–16272.
- (11) Zhuang, Z.; Shen, P.; Ding, S.; Luo, W.; He, B.; Nie, H.; Wang, B.; Huang, T.; Hu, R.; Qin, A.; Zhao, Z.; Tang, B. Z. Synthesis, Aggregation-Enhanced Emission, Polymorphism and Piezochromism of TPE-Cored Foldamers with Through-Space Conjugation. *Chem. Commun.* **2016**, *52*, 10842–10845.
- (12) Shen, P.; Jiao, S.; Zhuang, Z.; Dong, X.; Song, S.; Li, J.; Tang, B. Z.; Zhao, Z. Switchable Dual Circularly Polarized Luminescence in Through-Space Conjugated Chiral Foldamers. *Angew. Chem., Int. Ed.* **2024**, *63*, No. e202407605.
- (13) Xie, Y.; Liu, H.; Li, Z.; Zhang, X.; Song, L.; Zhou, K.; Yuan, F.; You, H.; Zhao, E.; He, Z. Construction of chiral through-space luminophores via symmetry breaking triggered by sequenced chlorination. *Sci. China Chem.* **2023**, *66*, 2083–2090.
- (14) Zhen, S.; Shen, P.; Li, J.; Zhao, Z.; Tang, B. Z. Giant Single-Molecule Conductance Enhancement Achieved by Strengthening Through-Space Conjugation with Thienyls. *Cell. Rep. Phys. Sci.* **2021**, *2*, No. 100364.
- (15) Zhen, S.; Mao, J. C.; Chen, L.; Ding, S.; Luo, W.; Zhou, X. S.; Qin, A.; Zhao, Z.; Tang, B. Z. Remarkable Multichannel Conductance of Novel Single-Molecule Wires Built on Through-Space Conjugated Hexaphenylbenzene. *Nano Lett.* **2018**, *18*, 4200–4205.
- (16) Chen, L.; Wang, Y. H.; He, B.; Nie, H.; Hu, R.; Huang, F.; Qin, A.; Zhou, X. S.; Zhao, Z.; Tang, B. Z. Multichannel Conductance of Folded Single-Molecule Wires Aided by Through-Space Conjugation. *Angew. Chem., Int. Ed.* **2015**, *54*, 4231–4235.
- (17) Li, J.; Zhuang, Z.; Shen, P.; Song, S.; Tang, B. Z.; Zhao, Z. Achieving Multiple Quantum-Interfered States via Through-Space and Through-Bond Synergistic Effect in Foldamer-Based Single-Molecule Junctions. *J. Am. Chem. Soc.* **2022**, *144*, 8073–8083.
- (18) Shen, P.; Liu, H.; Zhuang, Z.; Zeng, J.; Zhao, Z.; Tang, B. Z. Through-Space Conjugated Electron Transport Materials for Improving Efficiency and Lifetime of Organic Light-Emitting Diodes. *Adv. Sci. (Weinh.)* **2022**, *9*, No. 2200374.
- (19) Zhang, J.; Hu, L.; Zhang, K.; Liu, J.; Li, X.; Wang, H.; Wang, Z.; Sung, H. H. Y.; Williams, I. D.; Zeng, Z.; Lam, J. W. Y.; Zhang, H.; Tang, B. Z. How to Manipulate Through-Space Conjugation and Clusteroluminescence of Simple AIEgens with Isolated Phenyl Rings. *J. Am. Chem. Soc.* **2021**, *143*, 9565–9574.
- (20) Wang, L.; Xiong, Z.; Sun, J. Z.; Huang, F.; Zhang, H.; Tang, B. Z. How the Length of Through-Space Conjugation Influences the Clusteroluminescence of Oligo(Phenylene Methylenes). *Angew. Chem., Int. Ed.* **2024**, *63*, No. e202318245.
- (21) Han, Y.-Q.; Xie, Y.; Zhang, J.; Tan, S.; Zhang, H.; Tang, B. Z.; Sessler, J. L.; Huang, F. Fjord-Type AIEgens Based on Inherent Through-Space Conjugation. *CCS Chemistry*. **2024**, *6*, 1739–1747.
- (22) Luo, W.; Nie, H.; He, B.; Zhao, Z.; Peng, Q.; Tang, B. Z. Spectroscopic and Theoretical Characterization of Through-Space Conjugation of Foldamers with a Tetraphenylethene Hinge. *Chemistry*. **2017**, *23*, 18041–18048.
- (23) Hoffmann, R.; Imamura, A.; Hehre, W. J. Benzyne, Dehydroconjugated Molecules, and the Interaction of Orbitals Separated by  $\sigma$  Number of Intervening Bonds. *J. Am. Chem. Soc.* **1968**, *90*, 1499–1509.
- (24) Hoffmann, R. Interaction of Orbitals Through Space and Through Bonds. *Acc. Chem. Res.* **1971**, *4*, 1–9.
- (25) Brown, C. J.; Farthing, A. C. Preparation and Structure of Di-p-Xylylene. *Nature*. **1949**, *164*, 915–916.
- (26) Cram, D. J.; Allinger, N. L.; Steinberg, H. Macro Rings. VII. The Spectral Consequences of Bringing Two Benzene Rings Face to Face. *J. Am. Chem. Soc.* **1954**, *76*, 6132–6141.
- (27) Nozawa, R.; Kim, J.; Oh, J.; Lampert, A.; Wang, Y.; Shimizu, S.; Hisaki, I.; Kowalczyk, T.; Fliegl, H.; Kim, D.; Shinokubo, H. Three-Dimensional Aromaticity in an Antiaromatic Cyclophane. *Nat. Commun.* **2019**, *10*, 3576.
- (28) Bai, M.; Liang, J.; Xie, L.; Sanvito, S.; Mao, B.; Hou, S. Efficient Conducting Channels Formed by the  $\pi$ - $\pi$  Stacking in Single 2,2 Paracyclophane Molecules. *J. Chem. Phys.* **2012**, *136*, No. 104701.
- (29) Watanabe, M.; Goto, K.; Shibahara, M.; Shinmyozu, T. Synthesis, Structure, and Electronic and Photophysical Properties of Two- and Three-Layered [3.3]Paracyclophane-Based Donor-Acceptor Systems. *J. Org. Chem.* **2010**, *75*, 6104–6114.
- (30) Grimme, S.; Mück-Lichtenfeld, C. Accurate Computation of Structures and Strain Energies of Cyclophanes with Modern DFT Methods. *Isr. J. Chem.* **2012**, *52*, 180–192.
- (31) Sah, C.; Jacob, L.; Saraswat, M.; Venkataramani, S. Does a Nitrogen Lone Pair Lead to Two Centered-Three Electron (2c-3e) Interactions in Pyridyl Radical Isomers? *J. Phys. Chem. A* **2017**, *121*, 3781–3791.
- (32) Ivanov, M. V.; Wadumethrige, S. H.; Wang, D.; Rathore, R. Through-Space or Through-Bond? The Important Role of Cofaciality in Orbital Reordering and Its Implications for Hole (De)stabilization in Polychromophoric Assemblies. *J. Phys. Chem. C* **2017**, *121*, 15639–15643.
- (33) Jagtap, S. P.; Mukhopadhyay, S.; Coropceanu, V.; Brizius, G. L.; Bredas, J. L.; Collard, D. M. Closely Stacked Oligo(Phenylene Ethynylene)s: Effect of  $\pi$ -Stacking on the Electronic Properties of Conjugated Chromophores. *J. Am. Chem. Soc.* **2012**, *134*, 7176–7185.
- (34) Molina-Ontoria, A.; Wielopolski, M.; Gebhardt, J.; Gouloumis, A.; Clark, T.; Guldi, D. M.; Martin, N. [2,2']Paracyclophane-Based  $\pi$ -Conjugated Molecular Wires Reveal Molecular-Junction Behavior. *J. Am. Chem. Soc.* **2011**, *133*, 2370–2373.
- (35) Mo, Y.; Peyerimhoff, S. D. Theoretical analysis of electronic delocalization. *Journal of Chemical Physics*. **1998**, *109*, 1687–1697.
- (36) Yan, X.; Gao, H. A Theoretical Study on the Medicinal Properties and Electronic Structures of Platinum(IV) Anticancer Agents With Cl Substituents. *Front Oncol.* **2022**, *12*, No. 860159.
- (37) Battersby, T. R.; VernonClark, R.; Siegel, J. S. Does  $\pi$ - $\sigma$ - $\pi$  Through-Bond Coupling Significantly Increase C-C Bond Lengths? *J. Am. Chem. Soc.* **1997**, *119*, 7048–7054.
- (38) Mao, Y.; Loipersberger, M.; Horn, P. R.; Das, A.; Demerdash, O.; Levine, D. S.; Prasad Veccham, S.; Head-Gordon, T.; Head-Gordon, M. From Intermolecular Interaction Energies and Observable Shifts to Component Contributions and Back Again: A Tale of Variational Energy Decomposition Analysis. *Annu. Rev. Phys. Chem.* **2021**, *72*, 641–666.

- (39) Vermeeren, P.; van der Lubbe, S. C. C.; Fonseca Guerra, C.; Bickelhaupt, F. M.; Hamlin, T. A. Understanding chemical reactivity using the activation strain model. *Nat. Protoc.* **2020**, *15*, 649–667.
- (40) Su, P.; Chen, Z.; Wu, W. An Energy Decomposition Analysis Study for Intramolecular Non-Covalent Interaction. *Chem. Phys. Lett.* **2015**, *635*, 250–256.
- (41) Sutton, C.; Koerzdoerfer, T.; Gray, M. T.; Brunsfeld, M.; Parrish, R. M.; Sherrill, C. D.; Sears, J. S.; Bredas, J.-L. Accurate description of torsion potentials in conjugated polymers using density functionals with reduced self-interaction error. *J. Chem. Phys.* **2014**, *140*, No. 054310.
- (42) Nobuyasu, R. S.; Ward, J. S.; Gibson, J.; Laidlaw, B. A.; Ren, Z.; Data, P.; Batsanov, A. S.; Penfold, T. J.; Bryce, M. R.; Dias, F. B. The influence of molecular geometry on the efficiency of thermally activated delayed fluorescence. *J. Mater. Chem. C* **2019**, *7*, 6672–6684.
- (43) Zhao, Y.; Truhlar, D. G. Exploring the Limit of Accuracy of the Global Hybrid Meta Density Functional for Main-Group Thermochemistry, Kinetics, and Noncovalent Interactions. *J. Chem. Theory Comput.* **2008**, *4*, 1849–1868.
- (44) Josa, D.; Rodríguez-Otero, J.; Cabaleiro-Lago, E. M.; Rellán-Piñeiro, M. Analysis of the performance of DFT-D, M05–2X and M06–2X functionals for studying  $\pi\cdots\pi$  interactions. *Chem. Phys. Lett.* **2013**, *557*, 170–175.
- (45) Duan, Y.-C.; Gao, Y.; You, X.-X.; Wu, Y.; Geng, Y.; Fu, Y.-G.; Su, Z.-M. Theoretical study for the TADF nature of through-space conjugated [2.2]paracyclophane derivatives and the design for red-light emission. *Dyes Pigments*. **2022**, *202*, No. 110268.
- (46) Saleh, G.; Gatti, C.; Lo Presti, L. Energetics of Non-Covalent Interactions from Electron and Energy Density Distributions. *Comput. Theor. Chem.* **2015**, *1053*, 53–59.
- (47) Park, D.; Kang, S.; Ryoo, C. H.; Jhun, B. H.; Jung, S.; Le, T. N.; Suh, M. C.; Lee, J.; Jun, M. E.; Chu, C.; Park, J.; Park, S. Y. High-Performance Blue OLED using Multiresonance Thermally Activated Delayed Fluorescence Host Materials Containing Silicon Atoms. *Nat. Commun.* **2023**, *14*, 5589.
- (48) Meng, G.; Dai, H.; Wang, Q.; Zhou, J.; Fan, T.; Zeng, X.; Wang, X.; Zhang, Y.; Yang, D.; Ma, D.; Zhang, D.; Duan, L. High-Efficiency and Stable Short-Delayed Fluorescence Emitters with Hybrid Long- and Short-Range Charge-Transfer Excitations. *Nat. Commun.* **2023**, *14*, 2394.
- (49) Kasha, M.; Rawls, H. R.; Ashraf El-Bayoumi, M. *exciton model in molecular spectroscopy*. **1965**, *11*, 371–392.
- (50) Frisch, M. J.; Trucks, G. W.; Schlegel, H. B.; Scuseria, G. E.; Robb, M. A.; Cheeseman, J. R.; Scalmani, G.; Barone, V.; Petersson, G. A. et al. *Gaussian 16*; Gaussian Inc.: Wallingford, CT. 2016.
- (51) Tang, Z.; Song, Y.; Zhang, S.; Wang, W.; Xu, Y.; Wu, D.; Wu, W.; Su, P. XEDA, a fast and multipurpose energy decomposition analysis program. *J. Comput. Chem.* **2021**, *42*, 2341–2351.
- (52) Schmidt, M. W.; Baldridge, K. K.; Boatz, J. A.; Elbert, S. T.; Gordon, M. S.; Jensen, J. H.; Koseki, S.; Matsunaga, N.; Nguyen, K. A.; Su, S. J.; Windus, T. L.; Dupuis, M.; Montgomery, J. A. General Atomic and Molecular Electronic-Structure System. *J. Comput. Chem.* **1993**, *14*, 1347–1363.